

Nonuniform quantum well infrared photodetectors

S. Y. Wang and C. P. Lee

Citation: [Journal of Applied Physics](#) **87**, 522 (2000); doi: 10.1063/1.371893

View online: <http://dx.doi.org/10.1063/1.371893>

View Table of Contents: <http://scitation.aip.org/content/aip/journal/jap/87/1?ver=pdfcov>

Published by the [AIP Publishing](#)

Articles you may be interested in

[Quantum well infrared photodetectors hardiness to the nonideality of the energy band profile](#)

J. Appl. Phys. **107**, 123110 (2010); 10.1063/1.3446093

[Magnetic-field tunable terahertz quantum well infrared photodetector](#)

J. Appl. Phys. **98**, 084509 (2005); 10.1063/1.2085309

[Alloy scattering in GaAs/AlGaAs quantum well infrared photodetector](#)

J. Appl. Phys. **88**, 288 (2000); 10.1063/1.373655

[Current–voltage analysis of a tunneling emitter-undoped single quantum well infrared photodetector](#)

J. Appl. Phys. **87**, 8575 (2000); 10.1063/1.373581

[Noise characteristics of quantum-well infrared photodetectors at low temperatures](#)

Appl. Phys. Lett. **76**, 206 (2000); 10.1063/1.125703



Re-register for Table of Content Alerts

Create a profile.



Sign up today!



Nonuniform quantum well infrared photodetectors

S. Y. Wang and C. P. Lee^{a)}

Department of Electronic Engineering, National Chiao Tung University, Hsinchu, Taiwan, Republic of China

(Received 29 June 1999; accepted for publication 28 September 1999)

A nonuniform quantum well infrared photodetector (QWIP) structure is proposed. By changing the doping concentration and barrier width of each quantum well, the electric field distribution can be tailored. The nonuniform QWIPs show excellent performance compared with conventional uniform structures. The dark current is about an order of magnitude lower and the background limited temperature increases to 77 K. A detectivity of 2.0×10^{10} cm Hz^{1/2}/W and a responsivity of 0.25 A/W at 8.2 μ m have been obtained for these devices. A simple picture of electric field distribution within the structure is described to explain the results. © 2000 American Institute of Physics. [S0021-8979(00)07701-X]

I. INTRODUCTION

In the past decade, a great deal of effort has been put into the development of quantum well infrared photodetectors (QWIPs).¹ A large focal plane array with 640×468 pixels has recently been demonstrated.² The promising performance made QWIPs a good competitor to traditional HgCdTe detectors. However, despite all the advantages of QWIPs, they usually suffer from high dark current. So one is usually forced to operate the QWIPs below 77 K in order to meet the readout circuit requirement and to achieve the background limited operation.

In a conventional QWIP structure, the same quantum well and barriers are repeated many times. The whole absorption region, which consists of 30–50 identical quantum wells, is generally considered as a uniform active region. The optimization of the QWIP structure is usually concerned with the design of the quantum wells and the barriers but not the structure as a whole. However, some recent studies have revealed that the quantum wells cannot be treated the same.^{3–5} A self-consistent model based on the carrier capture probability and the emission probability has shown that the electric field distribution in the quantum well region is not uniform.⁴ The electric field in the first few barriers is much higher than that in the rest of the region. The depletion of the first few wells was also found, and it is the cause of the power nonlinearity of the responsivity at high voltages.⁵ So, it becomes clear that the electric field distribution can greatly change the QWIPs' characteristics.

In this work, we purposely use a nonuniform quantum well structure in a QWIP in order to alter the distribution of the electric field. The doping concentration and the barrier width is not the same for all the quantum wells in the new structure. Lower dark currents and higher gains were obtained with the new structure.

II. EXPERIMENTS

Samples used in this work were grown by MBE on a (100) semi-insulating GaAs substrate. For the nonuniform

structure, 35 periods of Al_{0.27}Ga_{0.73}As/GaAs quantum wells were used as the active region. As the growth progressed, the barrier width was increased from 150 to 850 Å, while the doping concentration in the well was decreased from 4×10^{18} to 5×10^{16} cm⁻³. The distributions of the doping concentration in the wells and the barrier width are shown in Fig. 1. Most of the doping concentration change was made in the first few wells (from 4×10^{18} to 6×10^{17} cm⁻³ for the first eight wells) and the barrier width changes linearly but more near the center of the active region. The width of all the quantum wells was kept at 45 Å. The Si dopants in each well were put in the center 25 Å region. The upper and bottom contact layers were 1 μ m *n*-type GaAs with a doping concentration of 2×10^{18} cm⁻³. For comparison, a standard sample with a uniform quantum well structure was also prepared. The barrier height and the well width were kept the same as the nonuniform structure to ensure the same absorption spectrum. The barrier width and the doping concentration of all the quantum wells were 500 Å and 6×10^{17} cm⁻³, respectively. The total sheet doping concentration and the barrier width were designed to be the same for both structures, so the absorbance of the samples was kept at the same value. The changes made in the nonuniform structure were to adjust the electric field distribution in the device.

After the layers were grown, the absorption spectra were measured by a FTIR using a 45° waveguide configuration. Almost the same absorption characteristics were obtained for both samples. After that, 200 μ m square mesas were defined and formed by chemical etching. Based on the absorption spectrum, which has a peak absorption at 8.4 μ m, stripe gratings with a 2.8 μ m period were fabricated to couple the normal incident infrared radiation. The gratings were etched into the top contact layer to a depth of 0.7 μ m. Au/Ge was put on the top and the bottom of the mesas for ohmic contacts.

After the devices were fabricated, dark current–voltage (*I*–*V*) characteristics at different temperatures and the 300 K background photocurrent at 10 K were measured using a close cycled helium cryostat. In all the measurements, the bottom contact is referenced as ground. As shown in Fig. 2,

^{a)}Electronic mail: cplee@cc.nctu.edu.tw

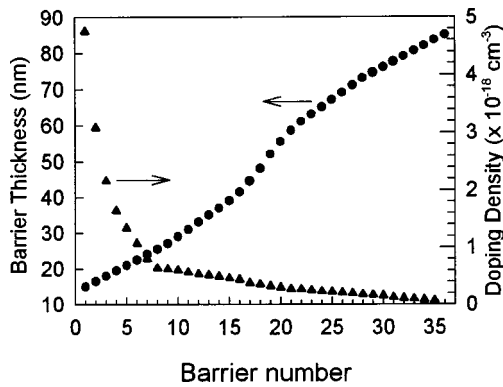


FIG. 1. The distributions of doping concentration and barrier width of each quantum well for the nonuniform sample.

the dark current of the nonuniform QWIP is about an order of magnitude lower than that of the normal structure. But the 300 K background photocurrent is almost the same (at forward bias). Because of the lower dark current, the BLIP temperature (with a field of view of 130°) of the new nonuniform QWIP is increased to 77 K, which is significantly higher than that (72 K) measured for the conventional uniform QWIP prepared side by side.

III. DISCUSSION

To understand why the dark current of the nonuniform QWIPs is lower, we need to know the electric field distribution in the devices. From the concept of current continuity

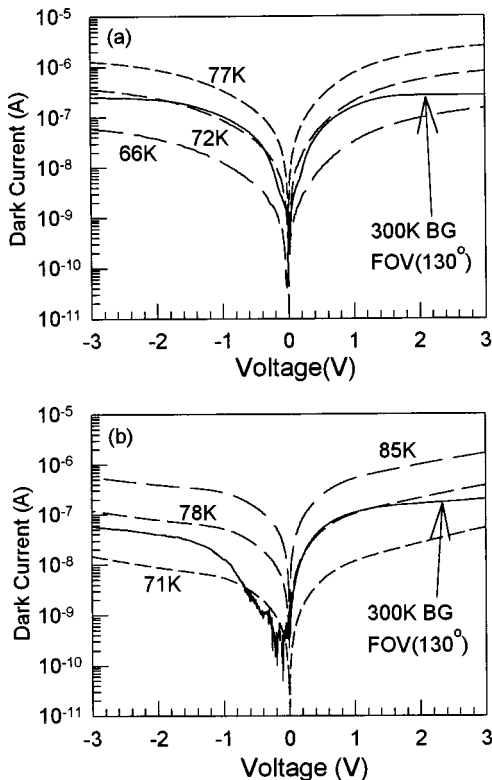


FIG. 2. The dark $I-V$ characteristics at different temperatures and the 300 K background photocurrent for: (a) a normal structure and (b) a nonuniform structure.

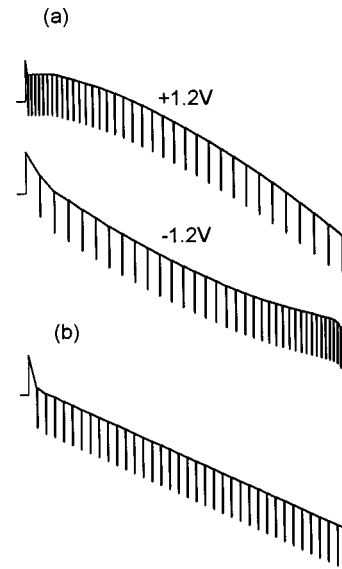


FIG. 3. The calculated voltage distribution of: (a) a nonuniform sample under positive and negative 1.2 V, (b) a uniform sample at 1.2 V.

and by balancing the number of carriers trapped by and the number of carriers escaped from each quantum well, the electric field distribution can be calculated.⁴ Figure 3(a) shows the calculated potential profiles of the nonuniform QWIP under a forward and reverse bias. For comparison, the potential distribution of a uniform structure is shown in Fig. 3(b). Because of the nonuniform doping and barrier width, the electric field in the new structure is quite nonuniform. In the highly doped region, the number of free carriers is high so the electric field is low. On the other hand, the lowly doped region has a high electric field.

Both Ref. 3 and 4 have calculated the electric field distribution in conventional QWIPs. Our calculated result on the uniform structure is very similar to that obtained in Ref. 4. In Ref. 3, however, they obtained a field distribution quite nonuniform even in a uniform structure. This is because they used only five wells and a much higher bias field than usual. In our calculation, in order to simulate realistic device operations, we used a realistic device structure under normal bias conditions. The nonuniform electric field can exist even at very small bias voltage for the nonuniform structure.

The effect of nonuniform field distribution on the dark current can be understood in the following way. Suppose the nonuniform structure consists of two regions with different doping concentrations as shown in Fig. 4. The free carrier concentrations (or the number of carriers that contributes to the dark current) in these two regions are n_1 and n_2 and the

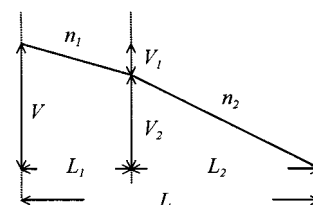


FIG. 4. The schematic diagram of the two region approximation of the nonuniform sample.

widths of the two regions are L_1 and L_2 . In the uniform structure, the free carrier concentration is n and the width is L . n_1 , n_2 , and n are obviously proportional to the respective doping concentrations. Since the total sheet doping densities of the two structures are the same, we have

$$n_1 L_1 + n_2 L_2 = nL.$$

If the total applied voltage is V , we have

$$V_1 + V_2 = V \quad \text{for } L_1 + L_2 = L.$$

The I - V relationships for the uniform and the nonuniform structures are

$$I = qn\mu V/L$$

and

$$I' = qn_1\mu V_1/L_1 = qn_2V_2/L_2,$$

respectively. Using these relationships, we can easily obtain the ratio between I and I' , which is

$$\frac{I}{I'} = \frac{L_1^2}{L^2} + \frac{L_2^2}{L^2} + \left(\frac{n_1}{n_2} + \frac{n_2}{n_1} \right) \frac{L_1 L_2}{L^2}.$$

Since

$$\frac{n_1}{n_2} + \frac{n_2}{n_1} \geq 2,$$

then

$$\frac{I}{I'} \geq \left(\frac{L_1}{L} + \frac{L_2}{L} \right)^2 = 1.$$

Therefore, we can see that the dark current of a uniform structure is higher than that of a nonuniform structure if they have the same total sheet carrier density. This is true for both forward and reverse bias conditions. In the simple model presented above, the free carrier concentrations n_1 and n_2 are proportional to n_w/L_B , where n_w is the carrier density in the quantum well and L_B is the barrier thickness. So, the electric field distribution depends on both n_w and L_B . However, based on our numerical simulation, the distribution of carrier density in the quantum wells plays a much more important role than the barrier thickness.

The photoresponse of the devices was measured at 77 K by a Fourier transform IR spectrometer, which was calibrated by a 1000 K blackbody source. The responsivity spectrum and the bias dependence of the response are shown in Fig. 5. Similar to the 300 K photocurrent, the bias dependence of responsivity is asymmetric. Although the dark current of this device is much lower, we found that the responsivity at forward bias is still very good and is about the same as that of the uniform structure. Normally, the photoresponse is higher for quantum wells with higher doping. In the new structure, the high doping wells are close to the cathode (in the forward bias case). However, as explained above, in this region the electric field is very small. So the electron's escape probability is small and the resulting quantum efficiency of these quantum wells also suffers. For the rest of the structure, since the average doping concentration is lower than that of the quantum wells in the uniform structure, the quantum efficiency is lower. Therefore the overall quantum

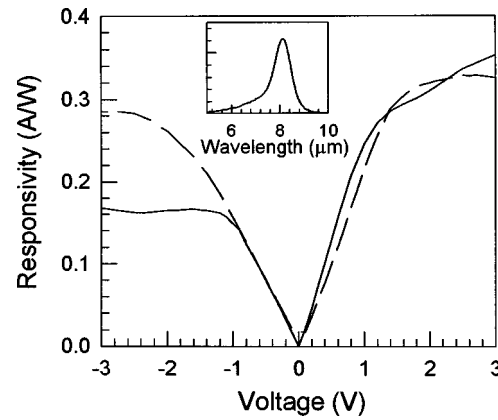


FIG. 5. The voltage dependence of responsivity of the samples. The solid line represents the responsivity of the nonuniform sample and the dashed line represents the responsivity of the uniform sample. The inset shows the responsivity spectrum of the nonuniform sample.

efficiency of the nonuniform structure should be lower than that of the uniform structure. The reason that we measured very good responsivity for the new structure is due to the increased gain in the device.

We have measured the noise spectral density of the devices. From the obtained noise i_n^2 and the dark current I_d , the gain can be calculated using the following relationship (assuming that the G - R noise dominates):

$$g_n = \frac{i_n^2}{4qI_d}.$$

The bias dependence of the noise gain for both samples is shown in Fig. 6. For the nonuniform QWIP, the gain increases with bias and saturates at a value of 1.5 at forward bias and 0.55 at reverse bias. For the normal uniform QWIP, the gain saturates at about 0.48. Therefore the new structure has a much higher gain in the forward direction compared to that of the conventional structure.

The increased gain in the nonuniform QWIP can also be understood from the electric field distribution in the device. As shown in Fig. 2, at a forward bias of 1.2 V, the electric field in the first few barriers (near the cathode) is nearly zero and then the electric field increases. Near the anode, the electric field becomes very large and is larger than 14 kV/cm.

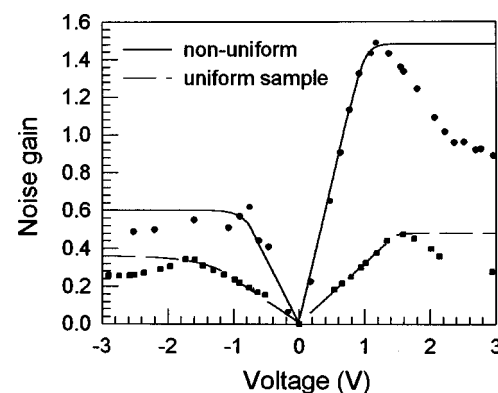


FIG. 6. The noise gain vs voltage plot for the two samples. The symbols represent the measured results and the lines are the fitting curves.

This strong field can induce impact ionization, which has been observed in n -type quantum wells.^{6,7} The electrons, which gain enough energy from the field, can interact with the confined electrons inside the quantum well to excite the carriers out of the well. This effect has been found in uniform QWIPs at large biases.⁸ Based on theoretical calculations,⁹ the threshold energy to induce impact ionization is about the same as the activation energy for the carriers in the quantum well and can be even lower if tunneling is taken into consideration. For the quantum well structure that we use, the activation energy is about 130 meV. In the region close to the anode, the barriers are quite thick (see Fig. 2). If we take the thickness of those barriers to be 800 Å, the electric field needed to induce ionization is about 16 kV/cm, so the impact ionization happens in this region. Under this situation, we have to re-examine the gain that we found from noise. The noise spectral density with the presence of impact ionization is

$$i_n^2 = 4qgI_d\Delta f \left[M^2 \left(2 - \frac{1}{M} \right) \right],$$

where M is the multiplication factor and g is the gain without multiplication. If we assume there is no impact ionization for the uniform QWIP (at least for voltages not too high), we can use the g value of the uniform QWIP in the above equation. If we take g to be 0.48, which is the saturated gain of the uniform QWIP, we obtain a multiplication factor of 1.5 at 1.2 V for the nonuniform QWIP using the above equation. For uniform QWIPs, the electric field is much more uniform. Under the same bias voltage of 1.2 V, the electric field is around 8 kV/cm, which is well below the threshold needed for impact ionization. When the nonuniform QWIP is reverse biased, the maximum electric field is also lower than that when it is forward biased. That is why the saturated gain is lower in the reverse direction.

As stated before, the electric field for the nonuniform QWIP under forward bias is nearly zero near the cathode. At such a low field, the electron's escape probability is around 0.45 for bound to continuum transitions.¹⁰ From the doping distribution shown in Fig. 1, the sheet doping density in this low field region is about $6.2 \times 10^{12} \text{ cm}^{-2}$. The rest of the structure is in the high field region, which has a sheet density of $3.3 \times 10^{12} \text{ cm}^{-2}$. The escape probability can be assumed to be 1. Since the sheet doping density in the whole structure is $9.5 \times 10^{12} \text{ cm}^{-2}$ for both the uniform structure and the nonuniform structure, the ratio of the overall quantum efficiencies for the two devices is

$$\frac{0.45 \times 6.2 \times 10^{12} + 3.3 \times 10^{12}}{9.5 \times 10^{12}} = 0.64.$$

Multiplying this number with the multiplication factor of 1.5, we then obtain a responsivity ratio of 0.96. This explains why we obtain a similar responsivity for the nonuniform QWIP (under forward bias) and the uniform QWIP.

So in our new structure, even when the quantum efficiency is lower (than that of the conventional structure) under forward bias, the responsivity is still good because of a higher gain. At higher biases, the multiplication factor continues to increase and the electron escape probability for higher doping wells also increases, so the responsivity can increase without saturation. This phenomenon can be seen in Fig. 5. We have measured the detectivity of the devices at 77 K. For the new nonuniform QWIP the detectivity is $2.0 \times 10^{10} \text{ cm Hz}^{1/2}/\text{W}$ at +1 V and maintains the same value to about 2.5 V. But for the normal structure, the detectivity is $1.2 \times 10^{10} \text{ cm Hz}^{1/2}/\text{W}$ at 1 V and decreases to $1.0 \times 10^{10} \text{ cm Hz}^{1/2}/\text{W}$ at 1.5 V.

IV. CONCLUSION

In conclusion, a nonuniform QWIP structure is described. By changing the doping concentration and barrier width of each well, the electric field distribution can be changed. The change in the electric field has a great influence on the detector's performance. The dark current is about an order of magnitude lower and the gain is significantly higher than those of the conventional uniform structure. The resulting detectivity is also higher and the BLIP temperature is increased to 77 K.

ACKNOWLEDGMENTS

The authors would like to thank Professor C. H. Kuan and M. C. Hsu of National Taiwan University for the noise measurements. This work is supported by the National Science Council under Contract No. NSC86-2215-E009-010.

¹B. F. Levine, J. Appl. Phys. **74**, R1 (1993).

²S. D. Gunapala, S. V. Bandara, J. K. Liu, W. Hong, M. Sundaram, P. D. Maker, R. E. Muller, C. A. Shott, and R. Carraalejo, IEEE Trans. Electron Devices **45**, 1890 (1998).

³M. Ershov, V. Ryzhii, and C. Hamaguchi, Appl. Phys. Lett. **67**, 3147 (1995).

⁴L. Thibaudeau, P. Bois, and J. Y. Duboz, J. Appl. Phys. **79**, 446 (1996).

⁵A. Sa'ar, C. Mermelstein, H. Schneider, C. Schoenbein, and M. Walther, in *Intrinsubband Transitions in Quantum Wells: Physics and Devices*, edited by S. S. Li and Y. K. Su (Kluwer Academic, 1998), p. 60.

⁶F. Capasso, J. Allam, A. Y. Cho, K. Mohammed, R. J. Malik, A. L. Hutchinson, and D. Sivco, Appl. Phys. Lett. **48**, 1294 (1986).

⁷M. Toivonen, M. Jalonen, A. Salokatve, and M. Pessa, Appl. Phys. Lett. **62**, 1664 (1993).

⁸B. F. Levine, K. K. Choi, C. G. Bethea, J. Walker, and R. J. Malik, Appl. Phys. Lett. **51**, 934 (1987).

⁹S. L. Chuang and K. Hess, J. Appl. Phys. **59**, 2885 (1986).

¹⁰B. F. Levine, A. Zussman, S. D. Gunapala, M. T. Asom, J. M. Kuo, and W. S. Hobson, J. Appl. Phys. **72**, 4429 (1992).